This is a preprint of an article published in Journal of Raman Spectroscopy

J. Raman Spectrosc. 2005; **36**: 116-122
Published online in Wiley Interscience (www.interscience.wiley.com). DOI: 10.1002/jrs.1292

Characterization of nonlinear optical superlattices by means of $\omega - \mathbf{k}$ spectroscopy

G.Kh.Kitaeva[1], V.V.Tishkova and A.N.Penin

M.V.Lomonosov Moscow State University, Faculty of Physics

Keywords: *second-order susceptibility, periodically poled, quasi-phase matching, non-linear photonic crystal*

---

[1]Correspondence to: G.Kh.Kitaeva, Chair of Quantum Electronics, Faculty of Physics, M.V.Lomonosov Moscow State University, 119992 Moscow Russia. Phone: 7(095)939 43 72, Fax: 7(095)939 11 04, E-mail: kit@qopt.phys.msu.su.

Sponsors: Russian Foundation for Basic Research (Grants 03-02-16364 and 02-02-16843), Grants for the leading scientific groups of Russia (No. 166.2003.02**)** and the Russian Federal Programs "Integration: Fundamental optics and spectroscopy", "Fundamental research in the field of physics: Development of the methods of optical spectroscopy with ultrahigh time resolution".

ABSTRACT

A method for measuring the spatial profiles of the second-order nonlinear susceptibility $\chi^{(2)}(z)$ in the bulk of periodically poled crystals and other structures was developed. The method is based on the general relation between the Fourier harmonics of $\chi^{(2)}(z)$ and the parametric signal line shape in the $\omega - \mathbf{k}$ space which is governed by the dependence of the output signal intensity on the phase mismatch. The special cases of nonlinear interferometers, and periodically poled crystals with the stepwise or smoothed space $\chi^{(2)}(z)$ profiles, and Fibonacci-type nonlinear superlattices were considered. The experimental schemes based on spontaneous parametric down-conversion and the second harmonic generation were compared and discussed.

1.Introduction.

The possibility for electromagnetic radiation frequency conversion is one of the major achievements of nonlinear optics. Two basic approaches are now used for the effective frequency conversion in a nonlinear medium: (1) matching phases of interacting waves using the optical birefringence [1], or (2) organizing quasi-synchronous processes using sign reversals of the second-order nonlinear susceptibility $\chi^{(2)}$ in nonlinear superlattices [2]. Presently, the second approach attracts a growing interest, since it enables to operate with the largest components of the $\chi^{(2)}$ tensor and to obtain collinear parametric processes in wider spectral ranges. One-dimensional nonlinear superlattices are intensively used in a quasi-phase matching regime for high-efficient frequency conversion [2-6], optical parametric generation [7-9], cascaded parametric processes [9-11], all-optical switching [12,13], and light squeezing [14,15]. In practice, these structures are formed in multidomain ferroelectric crystals, in which periodic or quasi-periodic reversals in the polar axis direction at the domain boundaries correlate with the sign reversals of the effective value of the nonlinear coefficient for a single domain [16]. The photonic band-gap structures with periodic linear susceptibility are currently attracting much attention also [17-19]. Coupled-mode equations for dielectric stacks of periodic linear and non-linear optical susceptibilities are usually considered numerically for the regime of high-gain parametric amplification and frequency conversion [18].

The problem of manufacturing and testing bulk regular multidomain structures is of current importance [20]. Mostly, the structure control consists of the imaging chemically etched surface of a multidomain crystal [21]. In the literature [22-24] there are methods based on the second harmonic generation, where nonlinear optical signals from different parts of the

internal structure volume are compared and analyzed. We propose a new method for the diagnostics of the spatial $\chi^{(2)}$ profile in the bulk of periodically and non-periodically poled crystals. The method is based on the analysis of the signal intensity dependence on the phase mismatch under the three-wave parametric interaction. A theoretical basis of this method is formulated in the Section 2 of this paper. Special cases of nonlinear interferometers, periodically poled crystals with the stepwise and smoothed space profiles of $\chi^{(2)}(z)$, quasi-periodic structures are considered. The Section 3 contains examples of the signal intensity distribution obtained experimentally for various periodically poled crystals in different parametric processes, spontaneous parametric down-conversion (SPDC) and second harmonic generation (SHG). The proposed schemes of diagnostics are discussed in the Section 4.

2. Parametric signal from a one-dimensional nonlinear superlattice as a function of the phase mismatch.

Consider the parametric interaction between three waves in a nonlinear multidomain crystal, where domains form a sequence of plane crystal layers with negative and positive orientation of polar axes. In each domain the convolution of polarization vectors of the waves with the components of the tensor $\hat{\chi}^{(2)}$ determines the effective value of nonlinear susceptibility $\chi^{(2)}$ for this process. Due to the symmetry breakdown at the domain boundaries, $\chi^{(2)}$ occurs to be different in positive and negative domains, in the central parts of domains and near their walls, and so on. In the general case, the one-dimensional spatial distribution of $\chi^{(2)}$ in these crystals is presented in the form of a Fourier-series as

$$\chi^{(2)}(\mathrm{z}) = \sum_{m=-\infty}^{\infty} \chi_m^{(2)} e^{\mathrm{imqz}}, \tag{1}$$

where $\chi_m^{(2)}$ are amplitudes of Fourier harmonics:

$$\chi_m^{(2)} = \frac{1}{\mathrm{d}} \int_{-d/2}^{d/2} \chi^{(2)}(\mathrm{z}) \exp(\text{-imqz}) \mathrm{dz}, \tag{2}$$

In the case of a periodic spatial $\chi^{(2)}(z)$ variation, d is period, **q** is the vector which characterizes the inverse nonlinear superlattice. For a non-periodic spatial $\chi^{(2)}(z)$ variation, d equals to the crystal thickness ℓ along the normal to domain layers. The direction of **q** is perpendicular to domain layers, $q=2\pi/\mathrm{d}$. Each harmonic of the m-th order determines an efficiency of a parametric process under the quasi-phase matching condition [2,25]:

$$\Delta\mathbf{k} - m\mathbf{q} = 0. \tag{3}$$

Here, $\Delta\mathbf{k} = \mathbf{k}_3 - (\mathbf{k}_1 \pm \mathbf{k}_2)$ is the phase mismatch for the considered parametric process, in which the frequencies of three waves are related as $\omega_3 = \omega_1 + \omega_2$ or as $\omega_3 = \omega_1 - \omega_2$. The changes in the linear optical susceptibility at the domain boundaries are usually negligibly small [26]. At the same time, there exists a possibility to achieve a highest modulation of $\chi^{(2)}(z)$ due to the reversals of the $\chi^{(2)}$ sign in periodically poled structures. As a result, the $\chi_{\pm 1}^{(2)}$ amplitudes of the same order as $\chi_0^{(2)}$ in a spatially uniform crystal are obtained. To set up an effective energy transfer between the waves, periodically poled structures are advantageous because of the quasi-phase matching conditions (3) are easy of access, instead of

the usual condition $\Delta\mathbf{k} = 0$. In most cases, for any given $\Delta\mathbf{k} \neq 0$ the proper period of domain poling is taken to satisfy (3).

While it was well known that the conversion efficiency is maximal in the directions given by (3), for a long time, in the literature there were no papers studying the overall distribution of the output signal intensity in different directions, for the whole possible range of phase mismatches $\Delta\mathbf{k}$. In [25], the theory of spontaneous and stimulated frequency conversion in a medium with arbitrary inhomogeneous one-dimensional $\chi^{(2)}$ distribution was developed. It was found that under conditions of low gain and constant pump, the intensity of the parametric signal is expressed explicitly in terms of phase mismatches and spatial Fourier harmonics $\chi_m^{(2)}$. When absorption at signal frequency ω_1, idler frequency ω_2, and pump frequency ω_3 considered to be negligible, the expression for the output signal intensity $P(\omega_1,\theta_1)$ can be written as follows:

$$P(\omega_1,\theta_1) = C_0 N_2(\omega_2,\theta_2)\left|\sum_{m=-\infty}^{\infty}\chi_m \mathrm{sinc}(\Delta_m/2)\right|^2 . \qquad (4)$$

Here $\Delta_m \equiv \ell\left(\Delta \mathrm{k}_z - mq\right)$ is the dimensionless projection of the quasi-phase mismatch $\Delta\mathbf{k} - m\mathbf{q}$ onto the normal to the domain layers. The factors $C_0 N_2(\omega_2,\theta_2)$ are the same as in the case of a homogenous nonlinear medium, where the signal distribution is described by the well-known expression

$$P(\omega_1,\theta_1) = C_0 N_2(\omega_2,\theta_2)\left[\chi \mathrm{sinc}(\Delta k\ell/2)\right]^2 . \qquad (4a)$$

$N_2(\omega_2,\theta_2)$ is the number of photons per each input idler mode inside the crystal (in the case

of SPDC, $N_2(\omega_2,\theta_2)$=1 [27]), C_0 is a common coefficient:

$$C_0 \equiv (\hbar\omega_1^4\omega_2/c^5 n_0 n_1 n_2)T_1\ T_3\ P_3\ell^2(\cos\theta_3\cos\theta_1/\cos\vartheta_3\cos\vartheta_1\cos\vartheta_2),$$

P_3 is the pump power, T_1 and T_3 are the transmission coefficients for the signal and pump waves at the crystal output and input surfaces, respectively, ϑ_i and θ_i are the angles of incidence inside and outside the crystal for the signal (i=1), idler (i=2) and pump (i=3) waves, determined by Snell's law. For the case of SHG, the pump and idler waves are the same and the corresponding coefficients take simpler forms. Usually, a nonlinear crystal is regarded as completely homogenous in directions normal to Z. Thus, the projection of the phase mismatch onto the domain layers $\Delta k_\perp$ should be equal to 0 if the transverse dimensions of the interacting beams are sufficiently large [28]. The exact phase matching condition $\Delta k_\perp$=0 determines a strict relation between the angles ϑ_1, ϑ_2, and ϑ_0 of the interacting monochromatic beams.

The third factor in (4), $I(\Delta) \equiv \left|\sum_{m=-\infty}^{\infty} \chi_m \mathrm{sinc}(\Delta_m/2)\right|^2$, depends directly on inhomogeneous behavior of the crystal nonlinear susceptibility. It describes the signal line shape under SPDC and under stimulated up- and down-conversion of the uniformly distributed input idler radiation (when $N_2(\omega_2,\theta_2)$=const). In principle, the measurement of $I(\Delta)$ provides the method to determine the Fourier harmonics χ_m and, finally, to reproduce the inhomogeneous distribution $\chi^{(2)}(z)$ by means of the Fourier transformation (1). Let us consider this line shape factor for different models of nonlinear superlattices.

a. Periodically poled multidomain crystal.

Each period of a periodic multidomain structure consists of two domains – the "positive" domain with the thickness ℓ_+ and the nonlinear susceptibility $\bar{\chi}$, and the "negative" domain with the thickness ℓ_- and the nonlinear susceptibility $-\bar{\chi}$. In the general case, there can be a narrow intermediate layer of thickness $2\Delta\ell$ between each pair of domain layers, in which $\chi^{(2)}$ is not constant and changes from $\bar{\chi}$ to $-\bar{\chi}$. The Fourier spectrum of such a structure can be simulated as

$$\chi_m = \frac{\bar{\chi}(-1)^{mn}}{\pi m}\left\{(-1)^m \sin m\pi\rho + i\left[(-1)^m \cos m\pi\rho - 1\right]\right\}\frac{\cos m\pi\delta}{\left[1-(2m\delta)^2\right]} \quad . \tag{5}$$

Here, the difference between domain thicknesses is characterized by the factor $\rho \equiv (\ell_+ - \ell_-)/d$, $\delta \equiv 2\Delta\ell/d$ is the relative thickness of the intermediate layer.

Practically, the thickness of the intermediate area is negligible in comparison with the domain thicknesses and, hence, $\delta \approx 0$. In this case, the signal line shape has the simple form

$$I(\Delta) = \frac{\bar{\chi}^2 \mathrm{sinc}^2(\Delta/2)}{\sin^2(\Delta/2n)}\left[1 - 2\cos\frac{\rho\Delta}{2n}\cos\frac{\Delta}{2n} + \cos^2\frac{\Delta}{2n}\right]. \tag{6}$$

Fig.1 illustrates the parametric signal line shape for asymmetric domain structures with different distinction between the domain thicknesses ρ. When ρ=0 ($\ell_+ = \ell_-$), the signal line shape contains odd-number maximums only. An asymmetry between the positive and negative domain thicknesses leads to the appearance of the even-number maximums also. When $|\rho|$ approaches its maximal value ($|\rho| \to 1$), the signal line shape transforms to the usual line shape of a homogeneous medium with the central peak at $\Delta = 0$.

The existence of rather thick intermediate layers, where the sign of $\chi^{(2)}$ changes, leads to the suppression of all maximums for which $|m|>1$. The relation between different-order peak values of $I(\Delta)$, measured for $\Delta=\Delta_m$, contains the information about the model parameters ρ and δ:

$$I_m \equiv I(\Delta_m) = (\bar{\chi}\rho)^2 \left[\frac{\cos m\pi\delta}{1-(2m\delta)^2}\right]^2 \times \begin{cases} \left[\dfrac{\cos(m\pi\rho/2)}{m\pi\rho/2}\right]^2 & \text{for odd m,} \\ \left[\dfrac{\sin(m\pi\rho/2)}{m\pi\rho/2}\right]^2 & \text{for even m.} \end{cases} \tag{7}$$

It is possible to determine these parameters by measuring relative intensities of quasi-synchronous maximums of different order.

b. Quasi-periodically poled multidomain crystal.

Quasi-periodically poled crystals can be treated by the similar approach. Consider the Fibonacci nonlinear optical superlattice [29-31]. It is a special sequence of building blocks A and B, each block consisting of one positive and one negative domain with susceptibilities $\bar{\chi}$ and $-\bar{\chi}$. The thicknesses of the building blocks A and B are $\ell_a = \ell_a^{(+)} + \ell_a^{(-)}$ and $\ell_b = \ell_b^{(+)} + \ell_b^{(-)}$. The structure parameter $\ell_a/\ell_b = \tau$ is taken as $\tau = \frac{1+\sqrt{5}}{2}$ below. The thicknesses of positive domains in different blocks are the same: $\ell_a^{(+)} = \ell_b^{(+)} \equiv \bar{\ell}$, but the thicknesses of negative domains are different: $\ell_a^{(-)} = \bar{\ell}(1+\eta)$, $\ell_a^{(+)} = \bar{\ell}(1-\tau\eta)$. The sequence of A and B is formed according to the rule $S_1 = A$, $S_2 = A|B$, $S_j = S_{j-1}|S_{j-2}$ for j>2. The dependence $\chi^{(2)}(z)$ in such structures is represented as a binary Fourier sequence [30]:

$$\chi(z)=\sum_{m=-\infty}^{\infty}\sum_{n=-\infty}^{\infty}\chi_{mn}e^{iG_{mn}z}. \qquad (8)$$

Here $G_{mn}=\frac{2\pi}{D}(m+n\tau)$, $\chi_{mn}=\overline{\chi}\times\mathrm{sinc}\frac{G_{mn}\overline{\ell}}{2}\times\mathrm{sinc}X_{mn}$, $D=\tau\ell_a+\ell_b$,

$X_{mn}=\frac{\pi\tau^2}{D}(m\ell_a-n\ell_b)$. The signal line shape is described by

$$I(\Delta)=\overline{\chi}^2\left|\sum_{m=-\infty}^{\infty}\sum_{n=-\infty}^{\infty}\mathrm{sinc}\frac{G_{mn}\overline{\ell}}{2}\times\mathrm{sinc}X_{mn}\times\mathrm{sinc}\frac{\Delta-G_{mn}\ell}{2}\right|^2 \qquad (9)$$

Signal line shapes calculated for 4 and 5 generations of the Fibonacci sequence, are presented in Fig.2.

c. Periodic stack of linear and nonlinear layers.

Several important structures can be presented as a periodic sequence of plane nonlinear layers of constant nonlinear susceptibility $\overline{\chi}$ and plane linear layers with $\chi^{(2)}$=0. If the linear-optical parameters do not vary in different layers, and absorption of idler waves is essential, and the thicknesses of linear and nonlinear layers are equal, then the signal line shape is represented as follows [32]:

$$I(\Delta)=\frac{4\overline{\chi}^2}{y_2^{\,2}+\Delta^2}\left\{\begin{array}{l}\left(e^{-y_2}\cos\Delta-1\right)\left[\frac{y_2^{\,2}-\Delta^2}{y_2^{\,2}+\Delta^2}\cdot\frac{1+\mathrm{ch}y_2'\cos\Delta'}{\left(\mathrm{ch}y_2'+\cos\Delta'\right)^2}-\frac{2y_2\Delta}{y_2^{\,2}+\Delta^2}\cdot\frac{\mathrm{sh}y_{22}'\sin\Delta'}{\left(\mathrm{ch}y_{22}'+\cos\Delta'\right)^2}\right]-\\ -e^{-y_2}\sin\Delta\cdot\left[\frac{2y_2\Delta}{y_2^{\,2}+\Delta^2}\cdot\frac{1+\mathrm{ch}y_2'\cos\Delta'}{\left(\mathrm{ch}y_2'+\cos\Delta'\right)^2}+\frac{y_2^{\,2}-\Delta^2}{y_2^{\,2}+\Delta^2}\cdot\frac{\mathrm{sh}y_{22}'\sin\Delta'}{\left(\mathrm{ch}y_{22}'+\cos\Delta'\right)^2}\right]+\\ +y_2-2n\cdot\left[\frac{y_2^{\,2}-\Delta^2}{y_2^{\,2}+\Delta^2}\cdot\frac{\mathrm{sh}y_2'}{\mathrm{ch}y_2'+\cos\Delta'}+2\frac{y_2\Delta}{y_2^{\,2}+\Delta^2}\cdot\frac{\sin\Delta'}{\mathrm{ch}y_{22}'+\cos\Delta'}\right]\end{array}\right\}. \qquad (10)$$

Here $y_2\equiv\alpha_2\ell/2\cos\vartheta_2$, α_2 is the absorption coefficient for idler waves, $\Delta'\equiv\Delta k\ell'$,

$y_2' \equiv \alpha_2 \ell' / 2\cos\vartheta_2$, ℓ' is the thickness of each layer.

The intensity distribution (10) is important for symmetric nonlinear interferometers [28,33]. Another example of a periodic stack can be obtained in a kind of periodic multidomain crystal where susceptibility $\chi^{(2)}$ is vanishingly small in each domain, but, due to a symmetry break-down, the sufficiently high values of $\chi^{(2)}$ ($\overline{\chi}$) are achieved at the domain boundaries. These structures are strongly asymmetric; the spectrum of periodic $\chi^{(2)}$ distribution may be written as $\chi_m \approx 2x(-1)^{mn}\,\overline{\chi}$, where x is a relative thickness of the nonlinear layers at the domain boundaries: $x \equiv 1-(\ell'/d) << 1$ (ℓ' is the thickness of each domain). In this case the signal line shape has the following form:

$$I(\Delta) = \frac{(x\overline{\chi})^2 n}{\left(\mathrm{ch}y_2' - \cos\Delta'\right)} \cdot \left\{ 4\mathrm{sh}y_2' + \frac{1}{2n\cdot\left(\mathrm{ch}y_2' - \cos\Delta'\right)} \left[\begin{array}{l} \left(e^{-y_2}\cos\Delta - 1\right)\left(\mathrm{sh}^2 y_2' - \sin^2\Delta'\right) + \\ +2e^{-y_2}\sin\Delta\sin\Delta'\mathrm{sh}y_2' \end{array} \right] \right\}. \quad (11)$$

Figure 3 shows the signal line shapes in nonlinear stacks with various differences between the thicknesses of linear (ℓ') and nonlinear (ℓ'') layers. The latter case is close to a limiting one and is described by (11).

d. Non-periodic structures.

Any inhomogeneous nonlinear media with an arbitrary non-periodical variation of $\chi^{(2)}(z)$ can be treated in the framework of the same approach also, conditionally being considered as one period of a periodic structure. The general expression (4) is valid if d is taken equal to the thickness of the whole structure ℓ.

There is another way to describe sequences of different uniform layers, developed in [34]. Further developing this approach, the relationship for a one-dimensional non-periodic stack of N layers can be calculated as:

$$I(\omega_1,\theta_1)=\frac{1}{\ell^2}\left|\sum_{j=1}^{N}\chi_j\ell_j\,\mathrm{sinc}(\Delta_j/2)e^{-i\Delta_j/2+i\sum_{j'=1}^{j}\Delta_{j'}}\right|^2. \qquad (12)$$

Here j is the number of the layer, χ_j is its nonlinear susceptibility, ℓ_j is its thickness, $\Delta_j\equiv\ell_j(\mathrm{k}_{1z}^{(j)}+\mathrm{k}_{2z}^{(j)}\pm\mathrm{k}_{3z}^{(j)})$ is the dimensionless phase mismatch in each layer (measured normally to the layers), $\mathrm{k}_i^{(j)}=\omega_i\,\mathrm{n}_i^{(j)}/c$ is the wave-vector of the signal (if i=1), idler (if i=2), or pump (if i=3) wave in the layer j, $\mathrm{n}_i^{(j)}$ is the corresponding refractive index of the j-th layer, $\ell=\sum_{j=1}^{N}\ell_j$ is the total thickness of the stack.

3. Measurement of the signal line shape of the second harmonic generation and the spontaneous parametric down-conversion.

Theoretically, any three-wave low-gain parametric processes can be used for the experimental measurement of the $I(\Delta)$ distribution. The stimulated and spontaneous processes, right up to the near-forward Raman scattering by phonon polaritons [35], can be considered as well. The main problem is obtaining signals corresponding to a large continuous variety of phase mismatch values Δ. In the layered structures, the transverse phase matching conditions $\Delta\mathrm{k}_\perp=0$ are usually satisfied. Thus, if the frequency and direction of the pump incidence are fixed, then for each pair of parameters ω_1,θ_1, characterizing the frequency and orientation of the signal output wave, one can indicate a pair of corresponding values of ω_2,θ_2 for the input idle wave and unambiguously calculate the value of mismatch Δ. To

change Δ, one should tune the signal parameters ω_1, θ_1, the idler parameters ω_2, θ_2, or the same pumping characteristics. In the case of SHG the two last groups coincide, since the idler and the pump waves are the same. Another problem arises when the stimulated processes are used. The inhomogeneous intensity distribution of the input idler radiation within the tuning ranges of angles and frequencies should be taken into account.

Figure 4 shows the signal line shape measured experimentally under the SHG of *oo-e* type in a periodically poled crystal layer of the total thickness 480 μm. The crystal layer was cut parallel to the z-axis and to domain surfaces, from the as-grown periodically poled crystal $LiNbO_3$:Y:Mg [36]. To tune the mismatch Δ we changed the incidence angle of the pump θ_3 under a constant pumping wavelength (1248 μm or 1254 μm). The values of $I(\Delta)$ were calculated from the measured SHG intensity $I_{SHG}(\theta_3)$, taking into account the reflection losses for pump and signal waves, as well as the variation of an effective nonlinear coefficient for each domain under the crystal rotation. Location of the main maximum at $\Delta = 2\pi \times (-8)$ indicates that there are 8 periods of the domain structure in the crystal layer, each period to be of $d \simeq 60\ \mu m$. Dotted line in Fig.4 shows the theoretical curve, which was calculated accounting the first harmonics only in (4). The comparison between this first approximation and the experimental results shows that the distribution of $\chi^{(2)}$ in the sample should be described by a larger spectrum of harmonics $\chi_m^{(2)}$. To estimate their values it is necessary to obtain the signal line shape in a wider range of phase mismatches.

The usage of stimulated processes enables one to study distribution of the signal intensity between the main peaks. In particular, here the distribution contains more detailed

information about domain structures. In case of SPDC, the signal intensity in these intervals is sufficiently lower than in the case of stimulated processes. Nevertheless, the SPDC-based schemes have a fundamental advantage: there is no necessity to use tunable sources of radiation at the crystal input. The idler modes are always uniformly occupied due to the zero vacuum fluctuations and the signals can be observed simultaneously within a very large range of mismatches Δ. An example of a two-dimensional spectrum of SPDC in a periodically poled crystal of $Ba_2NaNb_5O_{15}$ is presented in Fig.5, registered in coordinates $\{\lambda_1 \equiv 2\pi c/\omega_1, \theta_1\}$ by a photographic film at the exit of a spectrograph [37]. Different tuning curves correspond to different orders m of quasi-synchronous interaction. By measuring their positions, we have determined orientation and period of the domain superlattices with a rather high accuracy in previous works [37,38]. To obtain more detailed information about the internal distribution of $\chi^{(2)}$ it is necessary to analyze the precise intensity behavior $I(\Delta)$ across such spectra. The scanning of the mismatch Δ can be obtained here by scanning the signal frequency ω_1 or by scanning the signal angle θ_1.

4. Diagnostics of the spatial distribution of the second-order nonlinear susceptibility.

Basically, two approaches to determine the spatial $\chi^{(2)}$ distribution from the experimental signal line shape $I(\Delta)$ can be proposed. Based on a previous theoretical simulation**,** the first one can be applied if any certain prior information about the character of the $\chi^{(2)}$ distribution is available. For example, if one-dimensional and periodic character is ascertained for the $\chi^{(2)}$ distribution, one can determine the period, domain thicknesses and the

thickness of the intermediate layers using the relation (7) between different-order peak values of $I(\Delta)$.

The second approach, which is a more general one, can be used if the fitting is ineffective. It consists of the direct determination of the phases φ_m and the amplitudes χ_m of complex Fourier harmonics $\chi_m^{(2)} \equiv \chi_m e^{i\varphi_m}$. Since the values of $\chi^{(2)}$ are real, $\chi_m = \chi_{-m}$, φ_0=0, $\varphi_m = -\varphi_{-m}$. First, the relations between amplitudes χ_m are to be determined after measuring the intensities at points where quasi-phase mismatches are zero. As it follows from the general relation (4), all amplitudes χ_m can be expressed in terms of the maximal first-order harmonics

$$\chi_m / \chi_1 = \sqrt{I(2\pi mn)/I(2\pi n)}\,. \qquad (13)$$

Here, $n = \ell / d$, to be the number of periods in a periodic structure; $n = 1$ in a non-periodic structure. Second, the relations between the phases φ_m are to be determined by fitting the intensity behavior in the intervals between the quasi-synchronous maxima with the expression (4). A method of fitting depends on the results on amplitudes χ_m, which are obtained at the first step of the whole procedure. Finally, the spatial dependence of $\chi^{(2)}$ is to be reconstructed as $\chi^{(2)}(z)/\chi_1 = \sum_{m=-\infty}^{\infty} (\chi_m/\chi_1) e^{i(2\pi m+\varphi_m)z}$.

Conclusions.

We propose the method for measuring of the spatial $\chi^{(2)}(z)$ profiles in periodically poled structures by analysing the frequency/angular line shapes of low-gain parametric signals. The line shapes are governed by the signal intensity dependences on the wave mismatches, which are expressed in terms of Fourier harmonics of $\chi^{(2)}(z)$. The diagnostics of one-dimensional periodically, quasi-periodically, and non-periodically poled structures can be made by direct determining the Fourier spectrum of $\chi^{(2)}(z)$ or using the relationships, which we have obtained theoretically for a number of the most common models. For both approaches, it is necessary to measure the output signal intensity as a function of the phase mismatch under a three-wave parametric process. If the signal intensity exceeds the noise level, the use of the SPDC-based experimental schemes is more preferable, since the use of stimulated processes requires widely tunable sources of the input radiation whose non-uniform intensity distribution has to be taken into account. The developed approach can be applied for the study of spatial distribution of nonlinear susceptibilities in regular and non-regular multidomain ferroelectrics, in stochastic lamellar domain structures, sequences of domain walls, and for testing nonlinear photonic crystals.

Acknowledgments

The authors are grateful to Dr I.I.Naumova for growing and kindly supplying the crystal samples, to Prof. G.Yablonsky, Prof. M.V.Chekhova, Dr. K.A.Kuznetsov, and G.A.Maslennikov for the helpful remarks. This work was supported by the Russian Foundation for Basic Research (Grants 03-02-16364 and 02-02-16843), Grants for the leading scientific groups of Russia (No. 166.2003.02**)** and the Russian Federal Programs “Integration: Fundamental optics and spectroscopy”, “Fundamental research in the field of physics: Development of the methods of optical spectroscopy with ultrahigh time resolution”.

References

1. Shen Y.R. *The Principles of Nonlinear Optics*; Wiley: New York, 1984.

2. Byer R.L. *Nonlinear Optics* 1994; **7**: 235 . Byer R.L. *Journ. of Nonlinear Optical Physics & Materials* 1997; **6**: 549.

3. Lu Y., Mao L., Ming N. *Opt. Lett*. 1994; **19**: 1037.

4. Myers L.E., Miller G.D., Eckardt R.C., Fejer M.M., Byer R.L. *Opt. Lett*. 1995; **20**: 52.

5. Aleksandrovskii A.L., Volkov V.V. *Quantum Electronics* 1996; **23**: 542.

6. Bokhin A.V., Dmitriev V.G. *Quantum Electronics* 2002; **32**: 219.

7. Loza-Alvarez P., Brown C.T.A., Reid D.T., Sibbett W., Missey M. *Opt. Lett*. 1999; **24**: 1523.

8. Stothard D., Fortin P.-Y., Carleton A., Ebrahimzadeh M., Dunn M. *J. Opt. Soc. Am. B* 2003; **20**: 2102.

9. Chen D.-W. *J. Opt. Soc. Am. B* 2003; **20**: 1527.

10. Chirkin A.S., Volkov V.V., Laptev G.D., Morozov E.Yu. *Quantum Electronics* 2000; **30**: 847.

11. Kitaeva G.Kh., Mikhailovsky AA, Penin A.N. *JETP* 1997; **85**: 1094.

12. Asobe M., Yokohama I., Itoh H., Kaino T. *Opt. Lett*. 1997; **22**: 274.

13. Vidakovic P., Lovering D.J., Levenson J.A. *Opt. Lett*. 1997; **22**: 277.

14. Zhang K.S., Coudreau T., Martinelli M., Maitre A., Fabre C. *Phys.Rev.A* 2001; **64**:033815.

15. Serkland D.K., Fejer M.M., Byer R.L., Yamamoto Y. *Opt. Lett*. **20**, 1649 (1995).

16. Van der Ziel J.P., Bloembergen N. *Phys.Rev.* **135,** A1662 (1964).

17. *Development and Applications of Photonic Band Gap Materials*, edited by C.M.Bowden,

J.P.Dowling, and H.O.Everitt, special issue of *Opt. Soc. Am. B* 1993; **10**: 279-413.

18. Haus J.W., Soon B.Y., Scalora M., Sibilia C., Mel'nikov I.V. *J.Opt.Soc.Am.* 2002; **19**: 2282.
19. D'Aguanno G., Centini M., Scalora M., Sibilia C., Dumeige Y., Vidakovic P., Levenson J.A., Bloemer M.J., Bowden C.M., Haus J.W., Bertolotti M. *Phys.Rev.E* 2001; **64**: 016609.
20. Golenishev-Kutuzov A.V., Golenishev-Kutuzov V.A., Kalimullin R.I. *Physics-Uspekhi* 2000; **43**: 663.
21. Grilli S., Ferraro P., De Nicola S., Finizio A., Pierattini G., De Natale P., Chiarini M. *Optics Express* 2003; **11**: 392.
22. Holmgren S.J., Pasiskevicius V., Wang S., Laurell F. *Opt. Lett.* 2003; **28**: 1555.
23. Uesu Y., Kurimura S., Yamamoto Y. *Appl.Phys.Letts.* 1995; **66**: 2165.
24. Cudney R.S., Garces-Chavez V., Negrete-Regagnon P. *Opt. Lett*. 1997; **22**: 439.
25. Kitaeva G.Kh., Penin A.N. JETP; 2004; **98**:272.
26. A.L.Aleksandrovskii, Gliko O.A., Naumova I.I., Pryalkin V.I. *Quantum Electronics* 1996; **26**: 641.
27. Klyshko D.N. *Photons and Nonlinear Optics*; Gordon & Breach: 1987.
28. Burlakov A.V., Chekhova M.V., Klyshko D.N., Kulik S.P., Penin A.N., Shih Y.H., Strekalov D.V. Phys.Rev.A 1997; **56**: 3214.
29. Sibilia C., Tropea F., Bertolotti M. *J.Mod.Opt.* 1998; **45**: 2255.
30. Zhu S.N., Zhu Y.Y., Qin Y.Q., Wang H.F., Ge C.Z., Ming N.B. *Phys.Rev.Lett*. 1997; **78**: 2752.
31. Qin Y.Q., Su H., Tang S.H. *Appl.Phys.Lett.* 2003; **83:** 1071.
32. Kitaeva G.Kh., Penin A.N. *Quantum Electronics* 2004; **34**: 597.

33. Korystov D.Yu., Kulik S.P., Penin A.N. *JETP Lett.* 2001; **73**: 214.

34. Klyshko D.N. *JETP* 1993; **77**: 222.

35. Kitaeva G.Kh., Kulik S.P., Penin A.N. *Sov. Phys. Solid State* 1992; **34**:1841.

36. Naumova I.I., N.F.Evlanova, Gliko O.A., Lavrishchev S.V. *Journ. of Cryst. Growth* 1997; **181**: 160.

37. Aleksandrovskii A.A., Kitaeva G.Kh., Kulik S.P., Penin A.N. *Sov.Phys.JETP* 1986; **63**: 613.

38. Kitaeva G.Kh, Mikhailovsky A.A., Naumova I.I., Losevsky P.S., Penin A.N. *Appl.Phys.B* 1998; **66**: 201.

Figure captions

Fig.1. The signal line shape in a periodically poled crystal with unequal thicknesses of positive and negative domain, $\rho = (\ell_+ - \ell_-)/(\ell_+ + \ell_-)$, $\delta = 0$.

Fig.2. The signal line shape in a quasi-periodically poled crystal consisting of four and five generations of the Fibonacci sequence.

Fig.3. The signal line shapes in periodic stacks with different ratios between thicknesses of linear (ℓ') and nonlinear (ℓ'') layers, $\rho = (\ell'' - \ell')/(\ell' + \ell'')$.

Fig.4. The signal line shapes measured experimentally under SHG in the periodically poled crystal $LiNbO_3$:Y:Mg. Filled circles: pumping at 1.254 μm, open circles: pumping at 1.248 μm. Dotted line: calculations taking into account the first harmonics in (4).

Fig.5. SPDC spectrum of the multidomain crystal of $Ba_2NaNb_5O_{15}$.

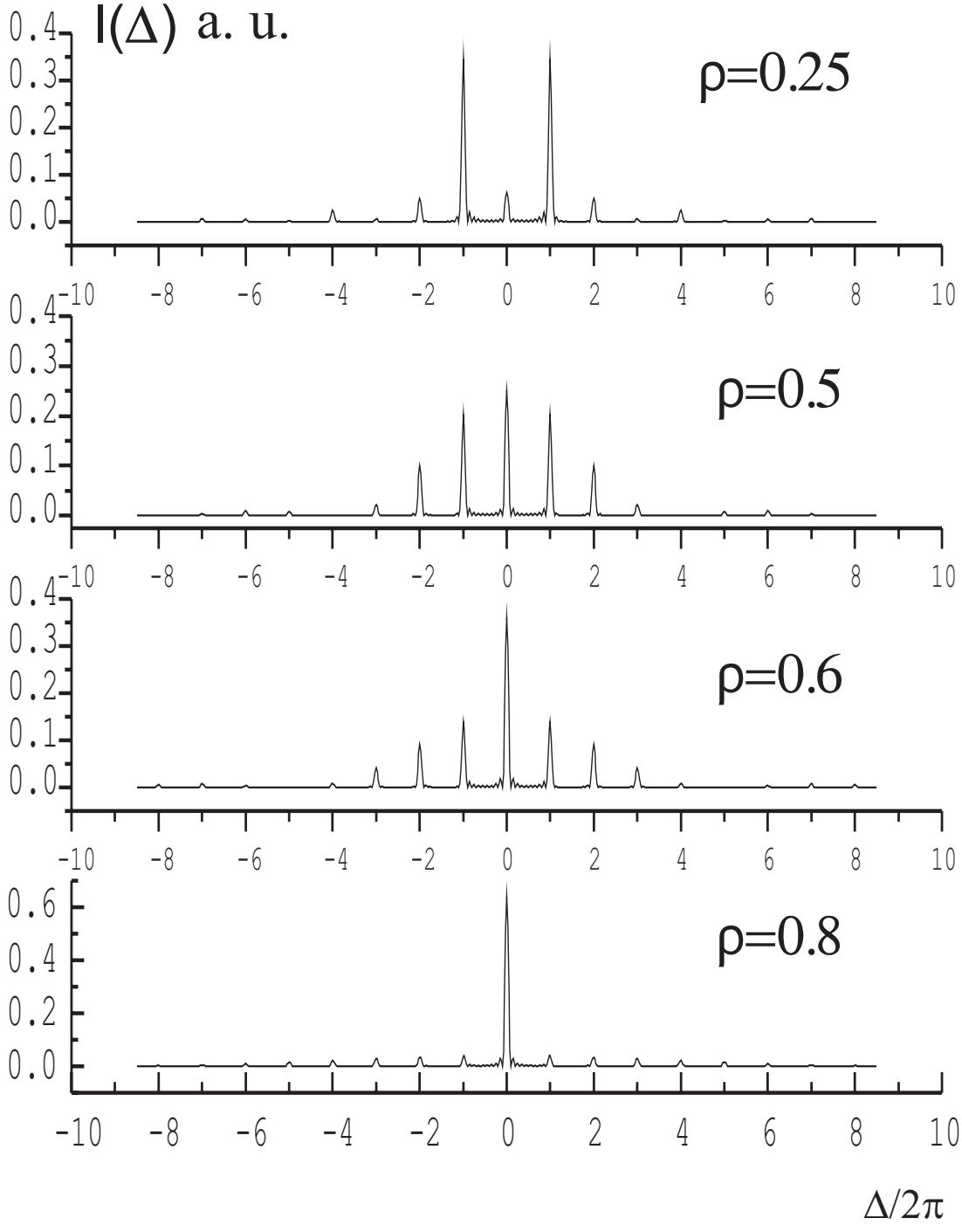
I(Δ) a. u.
ρ=0.25
ρ=0.5
ρ=0.6
ρ=0.8
0.4
0.3
0.2
0.1
0.0
0.6
0.4
0.2
0.0
-10
-8
-6
-4
-2
0
2
4
6
8
10
Δ/2π

Fig.1

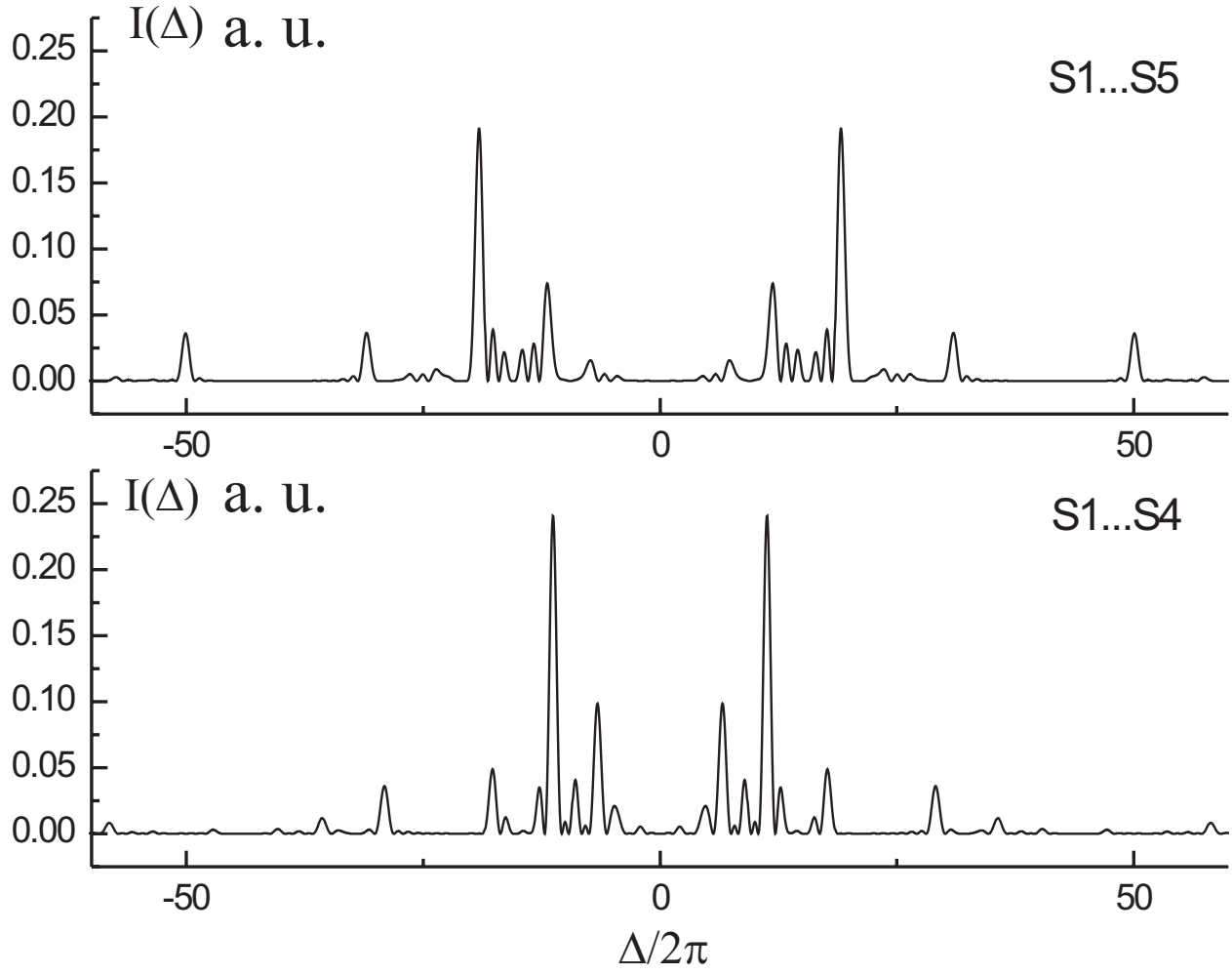
I(Δ) a. u.
S1...S5
0.25
0.20
0.15
0.10
0.05
0.00
-50
0
50
I(Δ) a. u.
S1...S4
0.25
0.20
0.15
0.10
0.05
0.00
-50
0
50
Δ/2π

Fig.2

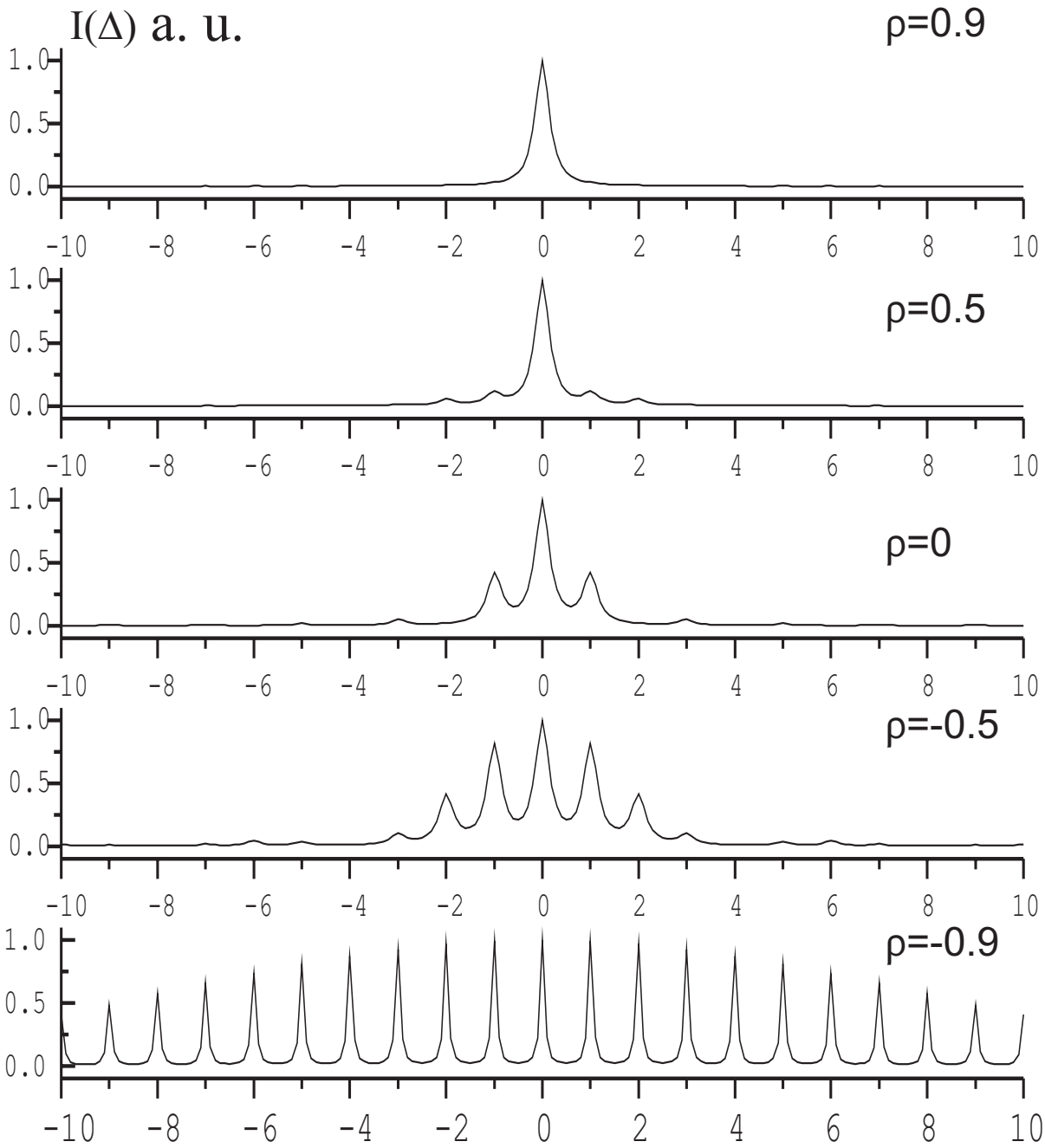

Fig.3

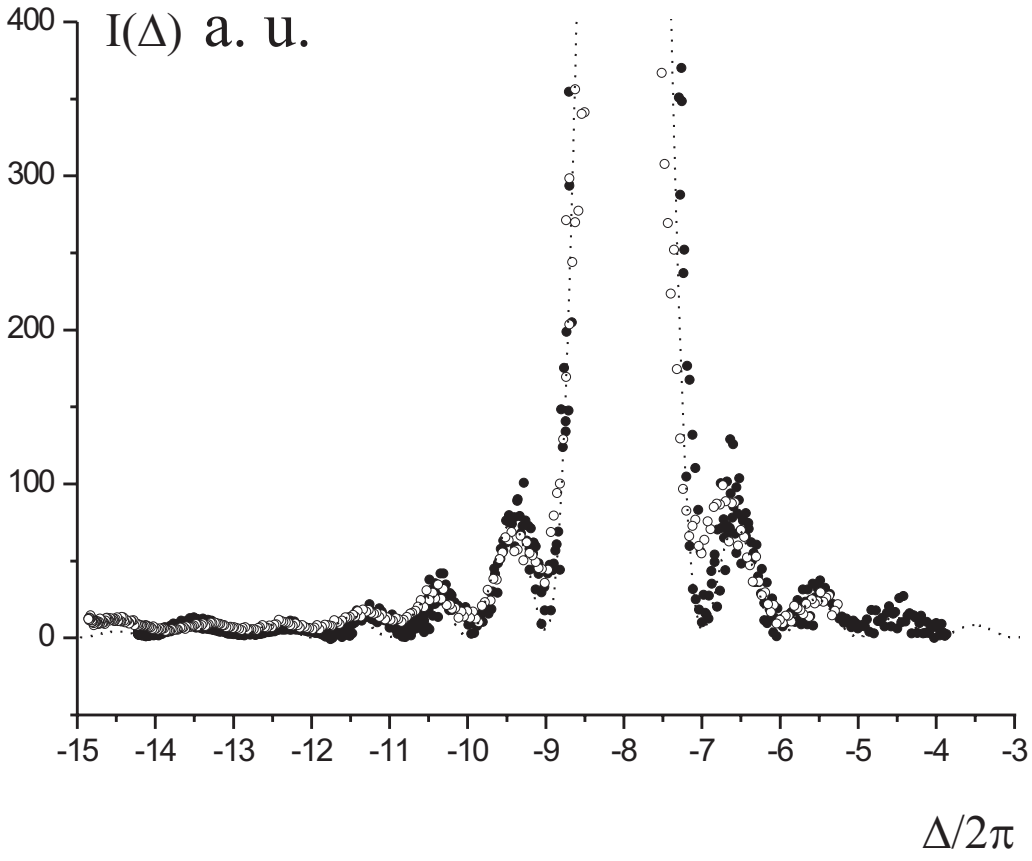

Fig.4

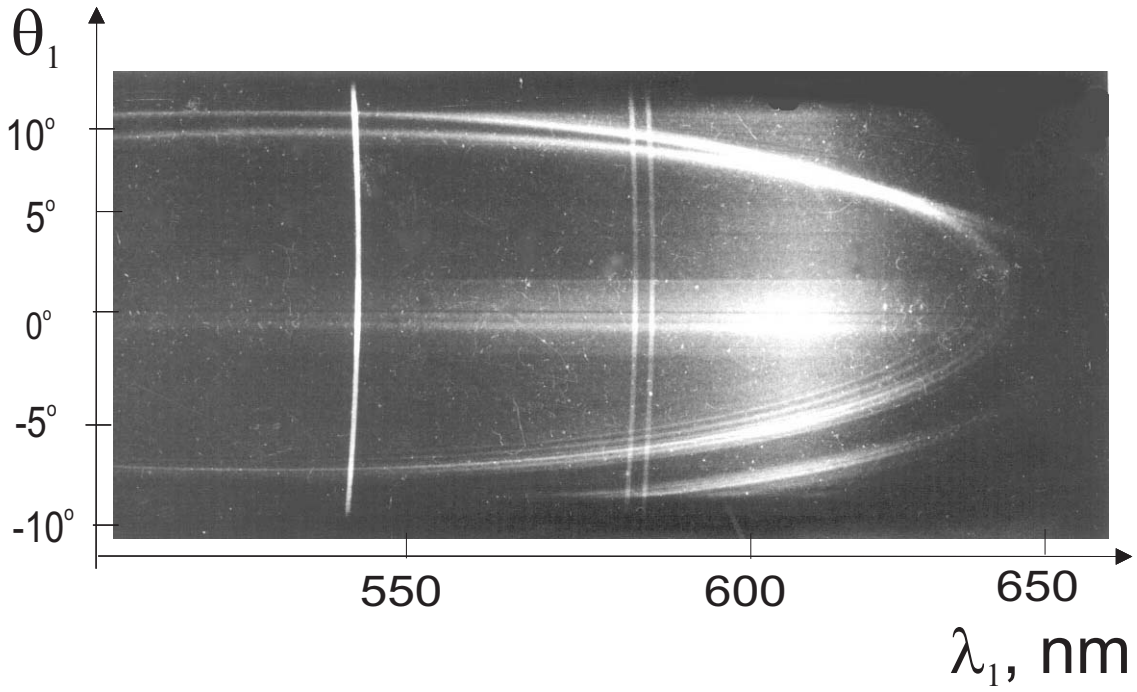

Fig.5